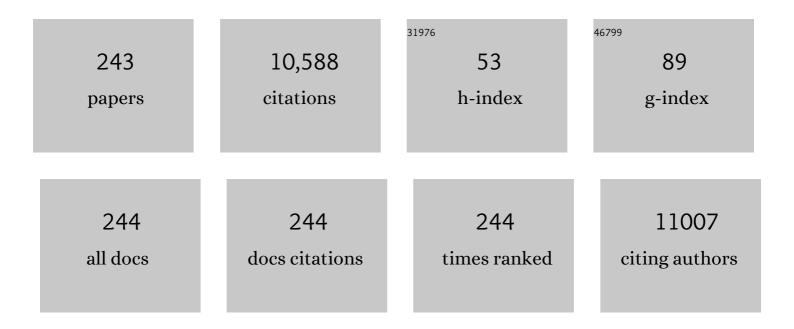
## Jie Zhang

List of Publications by Year in descending order

Source: https://exaly.com/author-pdf/8374925/publications.pdf Version: 2024-02-01



LE ZUANC

#	Article	IF	CITATIONS
1	Hierarchical Mesoporous SnO <sub>2</sub> Nanosheets on Carbon Cloth: A Robust and Flexible Electrocatalyst for CO <sub>2</sub> Reduction with High Efficiency and Selectivity. Angewandte Chemie - International Edition, 2017, 56, 505-509.	13.8	526
2	lonic liquids and their solid-state analogues as materials for energy generation and storage. Nature Reviews Materials, 2016, 1, .	48.7	511
3	Single-Boron Catalysts for Nitrogen Reduction Reaction. Journal of the American Chemical Society, 2019, 141, 2884-2888.	13.7	497
4	Towards a better Sn: Efficient electrocatalytic reduction of CO 2 to formate by Sn/SnS 2 derived from SnS 2 nanosheets. Nano Energy, 2017, 31, 270-277.	16.0	261
5	Conversion of dinitrogen to ammonia on Ru atoms supported on boron sheets: a DFT study. Journal of Materials Chemistry A, 2019, 7, 4771-4776.	10.3	251
6	Formation of lattice-dislocated bismuth nanowires on copper foam for enhanced electrocatalytic CO <sub>2</sub> reduction at low overpotential. Energy and Environmental Science, 2019, 12, 1334-1340.	30.8	230
7	Changing the Look of Voltammetry. Analytical Chemistry, 2005, 77, 186 A-195 A.	6.5	184
8	Architectural Design for Enhanced C <sub>2</sub> Product Selectivity in Electrochemical CO <sub>2</sub> Reduction Using Cu-Based Catalysts: A Review. ACS Nano, 2021, 15, 7975-8000.	14.6	183
9	Practical considerations associated with voltammetric studies in room temperature ionic liquids. Analyst, The, 2005, 130, 1132.	3.5	172
10	Unlocking the Electrocatalytic Activity of Antimony for CO <sub>2</sub> Reduction by Twoâ€Đimensional Engineering of the Bulk Material. Angewandte Chemie - International Edition, 2017, 56, 14718-14722.	13.8	164
11	Electrochemical maps and movies of the hydrogen evolution reaction on natural crystals of molybdenite (MoS <sub>2</sub> ): basal vs. edge plane activity. Chemical Science, 2017, 8, 6583-6593.	7.4	159
12	Polyethylenimine promoted electrocatalytic reduction of CO <sub>2</sub> to CO in aqueous medium by graphene-supported amorphous molybdenum sulphide. Energy and Environmental Science, 2016, 9, 216-223.	30.8	156
13	Electrochemical reduction of CO <sub>2</sub> on defect-rich Bi derived from Bi <sub>2</sub> S <sub>3</sub> with enhanced formate selectivity. Journal of Materials Chemistry A, 2018, 6, 4714-4720.	10.3	144
14	Controllable Synthesis of Few‣ayer Bismuth Subcarbonate by Electrochemical Exfoliation for Enhanced CO <sub>2</sub> Reduction Performance. Angewandte Chemie - International Edition, 2018, 57, 13283-13287.	13.8	141
15	Recent advances in the nanoengineering of electrocatalysts for CO <sub>2</sub> reduction. Nanoscale, 2018, 10, 6235-6260.	5.6	139
16	Conditions Required To Achieve the Apparent Equivalence of Adhered Solid- and Solution-Phase Voltammetry for Ferrocene and Other Redox-Active Solids in Ionic Liquids. Analytical Chemistry, 2003, 75, 2694-2702.	6.5	127
17	Graphene-supported [{Ru4O4(OH)2(H2O)4}(γ-SiW10O36)2]10â^' for highly efficient electrocatalytic water oxidation. Energy and Environmental Science, 2013, 6, 2654.	30.8	124
18	PdCu@Pd Nanocube with Pt-like Activity for Hydrogen Evolution Reaction. ACS Applied Materials & Interfaces, 2017, 9, 8151-8160.	8.0	114

#	Article	IF	CITATIONS
19	Utilization of nanoparticle labels for signal amplification in ultrasensitive electrochemical affinity biosensors: A review. Analytica Chimica Acta, 2013, 797, 1-12.	5.4	110
20	Voltammetric Determination of the Iodide/Iodine Formal Potential and Triiodide Stability Constant in Conventional and Ionic Liquid Media. Journal of Physical Chemistry C, 2015, 119, 22392-22403.	3.1	102
21	Is the Imidazolium Cation a Unique Promoter for Electrocatalytic Reduction of Carbon Dioxide?. Journal of Physical Chemistry C, 2016, 120, 23989-24001.	3.1	100
22	Electrocatalytic carbon dioxide reduction: from fundamental principles to catalyst design. Materials Today Advances, 2020, 7, 100074.	5.2	95
23	Theoretical Evaluation of Possible 2D Boron Monolayer in N <sub>2</sub> Electrochemical Conversion into Ammonia. Journal of Physical Chemistry C, 2018, 122, 25268-25273.	3.1	91
24	Two Tetra-Cd <sup>II</sup> -Substituted Vanadogermanate Frameworks. Journal of the American Chemical Society, 2014, 136, 5065-5071.	13.7	89
25	Voltammetric Studies on the Reduction of Polyoxometalate Anions in Ionic Liquids. Inorganic Chemistry, 2005, 44, 5123-5132.	4.0	83
26	Electrooxidation of Ethanol and Methanol Using the Molecular Catalyst [{Ru <sub>4</sub> O <sub>4</sub> (OH) <sub>2</sub> (H <sub>2</sub> O) <sub>4</sub> }(γ-SiW <sub>10Journal of the American Chemical Society, 2016, 138, 2617-2628.</sub>	>O <b>1su</b> b>3	6< <b>≴au</b> b>)≺sul
27	Ultrasensitive Electrochemical DNA Biosensors Based on the Detection of a Highly Characteristic Solid‣tate Process. Small, 2009, 5, 1414-1417.	10.0	80
28	Mechanistic understanding of the electrocatalytic CO2 reduction reaction – New developments based on advanced instrumental techniques. Nano Today, 2020, 31, 100835.	11.9	80
29	Fourier Transform Large-Amplitude Alternating Current Cyclic Voltammetry of Surface-Bound Azurin. Analytical Chemistry, 2004, 76, 166-177.	6.5	78
30	A DNA biosensor based on the detection of doxorubicin-conjugated Ag nanoparticle labels using solid-state voltammetry. Biosensors and Bioelectronics, 2009, 25, 282-287.	10.1	77
31	Porous nitrogen–doped carbon derived from biomass for electrocatalytic reduction of CO2 to CO. Electrochimica Acta, 2017, 245, 561-568.	5.2	76
32	Electrochemical Reduction of Carbon Dioxide in a Monoethanolamine Capture Medium. ChemSusChem, 2017, 10, 4109-4118.	6.8	75
33	Resistance, Capacitance, and Electrode Kinetic Effects in Fourier-Transformed Large-Amplitude Sinusoidal Voltammetry:  Emergence of Powerful and Intuitively Obvious Tools for Recognition of Patterns of Behavior. Analytical Chemistry, 2004, 76, 6214-6228.	6.5	73
34	NiO Nanoparticles Anchored on Phosphorusâ€Doped αâ€Fe <sub>2</sub> O <sub>3</sub> Nanoarrays: An Efficient Hole Extraction p–n Heterojunction Photoanode for Water Oxidation. ChemSusChem, 2018, 11, 2156-2164.	6.8	69
35	Large-Amplitude Fourier Transformed High-Harmonic Alternating Current Cyclic Voltammetry:Â Kinetic Discrimination of Interfering Faradaic Processes at Glassy Carbon and at Boron-Doped Diamond Electrodes. Analytical Chemistry, 2004, 76, 3619-3629.	6.5	67
36	Proton Diffusion at Phospholipid Assemblies. Journal of the American Chemical Society, 2002, 124, 2379-2383.	13.7	66

Jie Zhang

#	Article	IF	CITATIONS
37	An integrated instrumental and theoretical approach to quantitative electrode kinetic studies based on large amplitude Fourier transformed a.c. voltammetry: A mini review. Electrochemistry Communications, 2015, 57, 78-83.	4.7	66
38	Atomic nickel cluster decorated defect-rich copper for enhanced C2 product selectivity in electrocatalytic CO2 reduction. Applied Catalysis B: Environmental, 2021, 291, 120030.	20.2	66
39	Polyoxometalate-Promoted Electrocatalytic CO <sub>2</sub> Reduction at Nanostructured Silver in Dimethylformamide. ACS Applied Materials & Interfaces, 2018, 10, 12690-12697.	8.0	63
40	Two-Dimensional Boron Sheets as Metal-Free Catalysts for Hydrogen Evolution Reaction. Journal of Physical Chemistry C, 2018, 122, 19051-19055.	3.1	63
41	Discrimination and Evaluation of the Effects of Uncompensated Resistance and Slow Electrode Kinetics from the Higher Harmonic Components of a Fourier Transformed Large-Amplitude Alternating Current Voltammogram. Analytical Chemistry, 2007, 79, 2276-2288.	6.5	62
42	Pt nanoparticle label-mediated deposition of Pt catalyst for ultrasensitive electrochemical immunosensors. Biosensors and Bioelectronics, 2010, 26, 418-423.	10.1	62
43	CC Bond Formation <i>via</i> CH Activation and CN Bond Formation <i>via</i> Oxidative Amination Catalyzed by Palladium―Polyoxometalate Nanomaterials Using Dioxygen as the Terminal Oxidant. Advanced Synthesis and Catalysis, 2011, 353, 2988-2998.	4.3	62
44	Stannate derived bimetallic nanoparticles for electrocatalytic CO <sub>2</sub> reduction. Journal of Materials Chemistry A, 2018, 6, 7851-7858.	10.3	61
45	Microelectrochemical studies of charge transfer at the interface between two immiscible electrolyte solutions: electron transfer from decamethyl ferrocene to aqueous oxidants. Journal of Electroanalytical Chemistry, 2000, 483, 95-107.	3.8	60
46	Direct Detection of Electron Transfer Reactions Underpinning the Tin-Catalyzed Electrochemical Reduction of CO <sub>2</sub> using Fourier-Transformed ac Voltammetry. ACS Catalysis, 2017, 7, 4846-4853.	11.2	60
47	A critical assessment of electrochemistry in a distillable room temperature ionic liquid, DIMCARB. Green Chemistry, 2006, 8, 161-171.	9.0	59
48	Unlocking the Electrocatalytic Activity of Antimony for CO <sub>2</sub> Reduction by Twoâ€Dimensional Engineering of the Bulk Material. Angewandte Chemie, 2017, 129, 14910-14914.	2.0	58
49	Effect of Surface Pressure on the Insulator to Metal Transition of a Langmuir Polyaniline Monolayer. Journal of the American Chemical Society, 2003, 125, 9312-9313.	13.7	57
50	Facile electrochemical co-deposition of metal (Cu, Pd, Pt, Rh) nanoparticles on reduced graphene oxide for electrocatalytic reduction of nitrate/nitrite. Electrochimica Acta, 2018, 269, 733-741.	5.2	56
51	New Approach for Measuring Lateral Diffusion in Langmuir Monolayers by Scanning Electrochemical Microscopy (SECM):  Theory and Application. Journal of Physical Chemistry B, 2001, 105, 11120-11130.	2.6	55
52	Potential Dependence of Electron-Transfer Rates at the Interface between Two Immiscible Electrolyte Solutions:Â Reduction of 7,7,8,8-Tetracyanoquinodimethane in 1,2-Dichloroethane by Aqueous Ferrocyanide Studied with Microelectrochemical Techniques. Journal of Physical Chemistry B, 2000, 104, 2341-2347.	2.6	54
53	Electrochemical Studies on the Modular Podand 1,3,5-Tris(3-((ferrocenylmethyl)amino)pyridiniumyl)-2,4,6-triethylbenzene Hexafluorophosphate in Conventional Solvents and Ionic Liquids. Journal of Physical Chemistry B, 2003, 107, 5777-5786.	2.6	54
54	Prospects for a widely applicable reference potential scale in ionic liquids based on ideal reversible reduction of the cobaltocenium cation. Electrochemistry Communications, 2008, 10, 250-254.	4.7	54

#	Article	IF	CITATIONS
55	Voltammetric Reduction ofı́±- andı́³*-[S2W18O62]4-and ı̂±-, ı̂²-, and ı̂³-[SiW12O40]4-:Â Isomeric Dependence of Reversible Potentials of Polyoxometalate Anions Using Data Obtained by Novel Dissolution and Conventional Solution-Phase Processes. Inorganic Chemistry, 2004, 43, 8263-8271.	4.0	53
56	Voltammetric Determination of the Reversible Potentials for [{Ru <sub>4</sub> O <sub>4</sub> (OH) <sub>2</sub> (H <sub>2</sub> O) <sub>4</sub> }(γ-SiW <sub>10</sub> over the pH Range of 2–12: Electrolyte Dependence and Implications for Water Oxidation Catalysis. Inorganic Chemistry, 2013, 52, 11986-11996.	O <sub>4su</sub> b>36	،<الجناب: جزیر (sub) / sub
57	Direct Electrodeposition of Grapheneâ€Gold Nanocomposite Films for Ultrasensitive Voltammetric Determination of Mercury(II). Electroanalysis, 2014, 26, 121-128.	2.9	53
58	Voltammetric Ion-Selective Electrodes for the Selective Determination of Cations and Anions. Analytical Chemistry, 2010, 82, 1624-1633.	6.5	52
59	Fourier Transformed Large Amplitude Alternating Current Voltammetry: Principles and Applications. Review of Polarography, 2015, 61, 21-32.	0.1	52
60	The solid-state Ag/AgCl process as a highly sensitive detection mechanism for an electrochemical immunosensor. Chemical Communications, 2009, , 6231.	4.1	50
61	Simplifying the Evaluation of Graphene Modified Electrode Performance Using Rotating Disk Electrode Voltammetry. Langmuir, 2012, 28, 5275-5285.	3.5	50
62	Separation of Electron-Transfer and Coupled Chemical Reaction Components of Biocatalytic Processes Using Fourier Transform ac Voltammetry. Analytical Chemistry, 2005, 77, 3502-3510.	6.5	48
63	Higher Harmonic Large-Amplitude Fourier Transformed Alternating Current Voltammetry: Analytical Attributes Derived from Studies of the Oxidation of Ferrocenemethanol and Uric Acid at a Classy Carbon Electrode. Analytical Chemistry, 2008, 80, 4614-4626.	6.5	47
64	Facile electrochemical co-deposition of a graphene–cobalt nanocomposite for highly efficient water oxidation in alkaline media: direct detection of underlying electron transfer reactions under catalytic turnover conditions. Physical Chemistry Chemical Physics, 2014, 16, 19035-19045.	2.8	46
65	Synthesis, characterization and morphology of reduced graphene oxide–metal–TCNQ nanocomposites. Journal of Materials Chemistry C, 2014, 2, 870-878.	5.5	45
66	Stabilization of Lowâ€Valent Iron(I) in a Highâ€Valent Vanadium(V) Oxide Cluster. Angewandte Chemie - International Edition, 2017, 56, 14749-14752.	13.8	45
67	Electrocarboxylation of acetophenone in ionic liquids: the influence of proton availability on product distribution. Green Chemistry, 2014, 16, 2242-2251.	9.0	44
68	Mass-Transport and Heterogeneous Electron-Transfer Kinetics Associated with the Ferrocene/Ferrocenium Process in Ionic Liquids. Journal of Physical Chemistry C, 2016, 120, 16516-16525.	3.1	44
69	Selective electrochemical hydrogenation of furfural to 2-methylfuran over a single atom Cu catalyst under mild pH conditions. Green Chemistry, 2021, 23, 3028-3038.	9.0	43
70	Measurement of the forward and back rate constants for electron transfer at the interface between two immiscible electrolyte solutions using scanning electrochemical microscopy (SECM): Theory and experiment. Electrochemistry Communications, 2001, 3, 372-378.	4.7	42
71	Novel Kinetic and Background Current Selectivity in the Even Harmonic Components of Fourier Transformed Square-Wave Voltammograms of Surface-Confined Azurin. Journal of Physical Chemistry B, 2005, 109, 8935-8947.	2.6	42
72	Applications of Convolution Voltammetry in Electroanalytical Chemistry. Analytical Chemistry, 2014, 86, 2073-2081.	6.5	42

#	Article	IF	CITATIONS
73	Controllable Synthesis of Few‣ayer Bismuth Subcarbonate by Electrochemical Exfoliation for Enhanced CO <sub>2</sub> Reduction Performance. Angewandte Chemie, 2018, 130, 13467-13471.	2.0	42
74	Stepping towards Solar Water Splitting: Recent Progress in Bismuth Vanadate Photoanodes. ChemElectroChem, 2019, 6, 3227-3243.	3.4	42
75	Application of Power Spectra Patterns in Fourier Transform Square Wave Voltammetry To Evaluate Electrode Kinetics of Surface-Confined Proteins. Analytical Chemistry, 2006, 78, 2948-2956.	6.5	41
76	Advanced Composite 2D Energy Materials by Simultaneous Anodic and Cathodic Exfoliation. Advanced Energy Materials, 2018, 8, 1702794.	19.5	41
77	Selective laser sintering of TiO <sub>2</sub> nanoparticle film on plastic conductive substrate for highly efficient flexible dye-sensitized solar cell application. Journal of Materials Chemistry A, 2014, 2, 4566-4573.	10.3	40
78	Impact of Adsorption on Scanning Electrochemical Microscopy Voltammetry and Implications for Nanogap Measurements. Analytical Chemistry, 2016, 88, 3272-3280.	6.5	39
79	Rhodium-Catalyzed Hydroformylation of Alkenes Using in Situ High-Pressure IR and Polymer Matrix Techniques. Organometallics, 2003, 22, 1612-1618.	2.3	38
80	Theoretical studies of large amplitude alternating current voltammetry for a reversible surface-confined electron transfer process coupled to a pseudo first-order electrocatalytic process. Journal of Electroanalytical Chemistry, 2007, 600, 23-34.	3.8	38
81	Phosphomolybdic Acidâ€Assisted Growth of Ultrathin Bismuth Nanosheets for Enhanced Electrocatalytic Reduction of CO <sub>2</sub> to Formate. ChemSusChem, 2019, 12, 1091-1100.	6.8	38
82	Electron transfer reactions at gold nanoparticles. Chemical Communications, 2001, , 1818-1819.	4.1	37
83	Electrochemical Reduction of CO <sub>2</sub> at Metal Electrodes in a Distillable Ionic Liquid. ChemSusChem, 2016, 9, 1271-1278.	6.8	37
84	Mechanistic Analysis of the Electrocatalytic Properties of Dissolved α and β Isomers of [SiW12O40]4-and Solid [Ru(bipy)3]2[α-SiW12O40] on the Reduction of Nitrite in Acidic Aqueous Media. Inorganic Chemistry, 2006, 45, 3732-3740.	4.0	36
85	Detailed Analysis of the Electron-Transfer Properties of Azurin Adsorbed on Graphite Electrodes Using dc and Large-Amplitude Fourier Transformed ac Voltammetry. Analytical Chemistry, 2007, 79, 6515-6526.	6.5	36
86	Lindqvist Polyoxoniobate Ion-Assisted Electrodeposition of Cobalt and Nickel Water Oxidation Catalysts. ACS Applied Materials & amp; Interfaces, 2015, 7, 16632-16644.	8.0	35
87	Electroless deposition of iridium oxide nanoparticles promoted by condensation of [Ir(OH) <sub>6</sub> ] <sup>2â^'</sup> on an anodized Au surface: application to electrocatalysis of the oxygen evolution reaction. RSC Advances, 2015, 5, 3196-3199.	3.6	35
88	Recent advances and future perspectives for automated parameterisation, Bayesian inference and machine learning in voltammetry. Chemical Communications, 2021, 57, 1855-1870.	4.1	35
89	Large Amplitude Fourier Transformed AC Voltammetric Investigation of the Active State Electrochemistry of a Copper/Aqueous Base Interface and Implications for Electrocatalysis. Langmuir, 2011, 27, 10302-10311.	3.5	34
90	Detailed Electrochemical Studies of the Tetraruthenium Polyoxometalate Water Oxidation Catalyst in Acidic Media: Identification of an Extended Oxidation Series using Fourier Transformed Alternating Current Voltammetry. Inorganic Chemistry, 2012, 51, 11521-11532.	4.0	33

#	Article	IF	CITATIONS
91	Phosphomolybdate-doped-poly(3,4-ethylenedioxythiophene) coated gold nanoparticles: Synthesis, characterization and electrocatalytic reduction of bromate. Analytica Chimica Acta, 2013, 803, 41-46.	5.4	33
92	Electrode Reaction and Mass-Transport Mechanisms Associated with the Iodide/Triiodide Couple in the Ionic Liquid 1-Ethyl-3-methylimidazolium Bis(trifluoromethanesulfonyl)imide. Journal of Physical Chemistry C, 2014, 118, 22439-22449.	3.1	33
93	Electrochemical Hydrogenation of Furfural in Aqueous Acetic Acid Media with Enhanced 2â€Methylfuran Selectivity Using CuPd Bimetallic Catalysts. Angewandte Chemie - International Edition, 2022, 61, .	13.8	33
94	Comparison of Voltammetric Data Obtained for thetrans-[Mn(CN)(CO)2{P(OPh)3}(Ph2PCH2PPh2)]0/+Process in BMIM·PF6Ionic Liquid under Microchemical and Conventional Conditions. Analytical Chemistry, 2003, 75, 6938-6948.	6.5	32
95	Two Cobalt(II) 5-Aminoisophthalate Complexes and Their Stable Supramolecular Microporous Frameworks. Inorganic Chemistry, 2006, 45, 6276-6281.	4.0	32
96	Influences of the operative parameters and the nature of the substrate on the electrocarboxylation of benzophenones. Journal of Electroanalytical Chemistry, 2012, 664, 105-110.	3.8	32
97	Electrochemistry of Iodide, Iodine, and Iodine Monochloride in Chloride Containing Nonhaloaluminate Ionic Liquids. Analytical Chemistry, 2016, 88, 1915-1921.	6.5	32
98	Automatically Identifying Electrode Reaction Mechanisms Using Deep Neural Networks. Analytical Chemistry, 2019, 91, 12220-12227.	6.5	32
99	Resolution of coupled electron transfer–ion transfer processes at liquid/liquid interfaces by visualisation of interfacial concentration profiles. Chemical Communications, 1999, , 1501-1502.	4.1	31
100	The role of dissolution in the voltammetry of microdroplets and microparticles adhered to electrode surfaces in contact with aqueous electrolytes or ionic liquids. Journal of Electroanalytical Chemistry, 2005, 574, 299-309.	3.8	31
101	Applications of voltammetric ion selective electrodes to complex matrices. Analytical Methods, 2013, 5, 3840.	2.7	31
102	Phosphomolybdate@poly(diallyldimethylammonium chloride)-reduced graphene oxide modified electrode for highly efficient electrocatalytic reduction of bromate. Journal of Electroanalytical Chemistry, 2014, 727, 69-77.	3.8	31
103	Twoâ€Dimensional Electrocatalysts for Efficient Reduction of Carbon Dioxide. ChemSusChem, 2020, 13, 59-77.	6.8	31
104	Polyaniline Langmuir–Blodgett films: formation and properties. Physical Chemistry Chemical Physics, 2009, 11, 3490.	2.8	30
105	Modular Molecules: Siteâ€Selective Metal Substitution, Photoreduction, and Chirality in Polyoxometalate Hybrids. Chemistry - A European Journal, 2014, 20, 14102-14111.	3.3	30
106	Production of hydrogen peroxide in formulated beverages is associated with the presence of ascorbic acid combined with selected redox-active functional ingredients. Food Chemistry, 2021, 338, 127947.	8.2	30
107	Microelectrochemical measurements of electron transfer rates at the interface between two immiscible electrolyte solutions: Potential dependence of the ferro/ferricyanide-7,7,8,8-tetracyanoquinodimethane (TCNQ)/TCNQ˙– system. Physical Chemistry Chemical Physics. 2002. 4. 3820-3827.	2.8	29
108	Bioinspired Electrocatalytic CO <sub>2</sub> Reduction by Bovine Serum Albuminâ€Capped Silver Nanoclusters Mediated by [ <i>α</i> â€SiW <sub>12</sub> O <sub>40</sub> ] <sup>4â^'</sup> . ChemSusChem, 2016, 9, 80-87.	6.8	29

#	Article	lF	CITATIONS
109	Electrocatalytic CO <sub>2</sub> Reduction to Formate on Cu Based Surface Alloys with Enhanced Selectivity. ACS Sustainable Chemistry and Engineering, 2019, 7, 19453-19462.	6.7	29
110	Scanning electrochemical microscopy (SECM) feedback approach for measuring lateral proton diffusion in langmuir monolayers: theory and application. Physical Chemistry Chemical Physics, 2002, 4, 3814-3819.	2.8	28
111	Investigation of Mediated Oxidation of Ascorbic Acid by Ferrocenemethanol Using Large-Amplitude Fourier Transformed ac Voltammetry under Quasi-Reversible Electron-Transfer Conditions at an Indium Tin Oxide Electrode. Analytical Chemistry, 2008, 80, 6515-6525.	6.5	28
112	Fourier transformed alternating current voltammetry in electromaterials research: Direct visualisation of important underlying electron transfer processes. Current Opinion in Electrochemistry, 2018, 10, 72-81.	4.8	28
113	Electrodeposition of lead on glassy carbon and mercury film electrodes from a distillable room temperature ionic liquid, DIMCARB. Journal of Solid State Electrochemistry, 2007, 11, 1593-1603.	2.5	27
114	Electrode Kinetics Associated with Tetracyanoquinodimethane (TCNQ), TCNQ <sup>•–</sup> , and TCNQ <sup>2–</sup> Redox Chemistry in Acetonitrile As Determined by Analysis of Higher Harmonic Components Derived from Fourier Transformed Large Amplitude ac Voltammetry. Journal of Physical Chemistry C, 2011, 115, 24153-24163.	3.1	27
115	Synthesis and structure of a novel open-framework zincophosphate with intersecting three-dimensional helical channels. Dalton Transactions RSC, 2002, , 4527.	2.3	26
116	Combined scanning electrochemical microscopy–Langmuir trough technique for investigating phase transfer kinetics across liquid/liquid interfaces modified by a molecular monolayer. Electrochemistry Communications, 2003, 5, 105-110.	4.7	26
117	Mediator Enhanced Water Oxidation Using Rb <sub>4</sub> [Ru <sup>II</sup> (bpy) <sub>3</sub> ] <sub>5</sub> [{Ru <sup>III</sup> <sub>4</sub> O <sub> Film Modified Electrodes. Inorganic Chemistry, 2014, 53, 7561-7570.</sub>	∘4< <i>⊭</i> ⊾oob>(C	)H)₂csub>2∢
118	Cobalt selenide nanoflake decorated reduced graphene oxide nanocomposite for efficient glucose electro-oxidation in alkaline medium. Journal of Materials Chemistry A, 2017, 5, 19289-19296.	10.3	26
119	Use of Bayesian Inference for Parameter Recovery in DC and AC Voltammetry. ChemElectroChem, 2018, 5, 917-935.	3.4	26
120	Advanced Spatiotemporal Voltammetric Techniques for Kinetic Analysis and Active Site Determination in the Electrochemical Reduction of CO <sub>2</sub> . Accounts of Chemical Research, 2022, 55, 241-251.	15.6	26
121	Kinetics of IrCl62- Ion Transfer across the Water/1,2-Dichloroethane Interface and the Effect of a Phospholipid Monolayer. Langmuir, 2002, 18, 2313-2318.	3.5	25
122	A unique proton coupled electron transfer pathway for electrochemical reduction of acetophenone in the ionic liquid [BMIM][BF4] under a carbon dioxide atmosphere. Green Chemistry, 2011, 13, 3461.	9.0	25
123	Bismuth Vanadate with Electrostatically Anchored 3D Carbon Nitride Nanoâ€networks as Efficient Photoanodes for Water Oxidation. ChemSusChem, 2018, 11, 2510-2516.	6.8	25
124	Effect of Fatty Alcohol Monolayers on the Rate of Bromine Transfer across the Water/Air Interface: Assessment of Candidate Models Using Scanning Electrochemical Microscopy. Langmuir, 2002, 18, 1218-1224.	3.5	24
125	Fourier Transformed Large Amplitude Square-Wave Voltammetry as an Alternative to Impedance Spectroscopy: Evaluation of Resistance, Capacitance and Electrode Kinetic Effects via an Heuristic Approach. Electroanalysis, 2005, 17, 1450-1462.	2.9	24
126	Concentration and electrode material dependence of the voltammetric response of iodide on platinum, glassy carbon and boron-doped diamond in the room temperature ionic liquid 1-ethyl-3-methylimidazolium bis(trifluoromethanesulfonyl)imide. Electrochimica Acta, 2013, 109, 554-561.	5.2	24

#	Article	IF	CITATIONS
127	Mass Transport Studies and Hydrogen Evolution at a Platinum Electrode Using Bis(trifluoromethanesulfonyl)imide as the Proton Source in Ionic Liquids and Conventional Solvents. Journal of Physical Chemistry C, 2014, 118, 29663-29673.	3.1	24
128	Comparison of fast electron transfer kinetics at platinum, gold, glassy carbon and diamond electrodes using Fourier-transformed AC voltammetry and scanning electrochemical microscopy. Physical Chemistry Chemical Physics, 2017, 19, 8726-8734.	2.8	24
129	Microelectrochemical Measurements at Expanding Droplets:  Effect of Surfactant Adsorption on Electron Transfer Kinetics at Liquid/Liquid Interfaces. Langmuir, 2001, 17, 821-827.	3.5	23
130	Study of the reaction of Rh(acac)(CO)2 with alkenes in polyethylene films under high-pressure hydrogen and the Rh-catalysed hydrogenation of alkenes. Journal of Organometallic Chemistry, 2003, 678, 128-133.	1.8	23
131	Electrochemical Proton Reduction and Equilibrium Acidity (p <i>K</i> <sub>a</sub> ) in Aprotic Ionic Liquids: Protonated Amines and Sulfonamide Acids. Journal of Physical Chemistry C, 2015, 119, 21828-21839.	3.1	23
132	Effect of phospholipids on the kinetics of dioxygen transfer across a 1,2-dichloroethane/water interface. Physical Chemistry Chemical Physics, 2001, 3, 5553-5558.	2.8	22
133	Ultrasensitive electrochemical immunosensor employing glucose oxidase catalyzed deposition of gold nanoparticles for signal amplification. Biosensors and Bioelectronics, 2011, 27, 53-57.	10.1	22
134	Advantages Available in the Application of the Semi-Integral Electroanalysis Technique for the Determination of Diffusion Coefficients in the Highly Viscous Ionic Liquid 1-Methyl-3-Octylimidazolium Hexafluorophosphate. Analytical Chemistry, 2013, 85, 2239-2245.	6.5	22
135	Electrochemical Reduction of CO <sub>2</sub> with an Oxideâ€Derived Lead Nanoâ€Coralline Electrode in Dimcarb. ChemElectroChem, 2017, 4, 1402-1410.	3.4	22
136	Unexpected Complexity in the Electro-Oxidation of Iodide on Gold in the Ionic Liquid 1-Ethyl-3-methylimidazolium bis(trifluoromethanesulfonyl)imide. Analytical Chemistry, 2013, 85, 11319-11325.	6.5	21
137	Diminished Electron Transfer Kinetics for [Ru(NH <sub>3</sub> ) <sub>6</sub> ] <sup>3+/2+</sup> , [α-SiW <sub>12</sub> O <sub>40</sub> ] <sup>4–/5–</sup> , and [α-SiW <sub>12</sub> O <sub>40</sub> ] <sup>5–/6–</sup> Processes at Boron-Doped Diamond Electrodes. Journal of Physical Chemistry C, 2015, 119, 12464-12472.	3.1	21
138	Dual-Frequency Alternating Current Designer Waveform for Reliable Voltammetric Determination of Electrode Kinetics Approaching the Reversible Limit. Analytical Chemistry, 2016, 88, 2367-2374.	6.5	21
139	Scanning Electrochemical Microscopy (SECM) Studies of Oxygen Transfer across Phospholipid Monolayers under Surface Pressure Control:Â Comparison of Monolayers at Air/Water and Oil/Water Interfaces. Langmuir, 2004, 20, 701-707.	3.5	20
140	AFM study of morphological changes associated with electrochemical solid–solid transformation of three-dimensional crystals of TCNQ to metal derivatives (metal = Cu, Co, Ni;) Tj ETQq0 0 0 rgBT /Overloc	k <b>2.6</b> Tf 5(	0 22107 Td (TC
141	Polystyrenesulfonate doped poly(Hydroxymethyl 3,4-Ethylenedioxythiophene) stabilized Au nanoparticle modified glassy carbon electrode as a reusable sensor for mercury(II) detection in chloride media. Journal of Electroanalytical Chemistry, 2013, 704, 96-101.	3.8	20
142	Cobalt(II) phosphonate coordination polymers: Synthesis, characterization and application as oxygen evolution electrocatalysts in aqueous media and water-saturated hydrophobic 1-butyl-3-methylimidazolium hexafluorophosphate ionic liquid. Electrochimica Acta, 2013, 101, 201-208.	5.2	20
143	Large-Amplitude Fourier-Transformed AC Voltammetric Study of the Capacitive Electrochemical Behavior of the 1-Butyl-3-methylimidazolium Tetrafluoroborate–Polycrystalline Gold Electrode Interface. Journal of Physical Chemistry C, 2017, 121, 12136-12147.	3.1	20
144	Identification of a new substrate effect that enhances the electrocatalytic activity of dendritic tin in CO2 reduction. Physical Chemistry Chemical Physics, 2018, 20, 5936-5941.	2.8	20

#	Article	IF	CITATIONS
145	Electrochemistry of nickel(II) and copper(II) N,N′-ethylenebis(acetylacetoniminato) complexes and their electrocatalytic activity for reduction of carbon dioxide and carboxylic acid protons. Transition Metal Chemistry, 2014, 39, 819-830.	1.4	19
146	Electrochemical reduction of aromatic ketones in 1-butyl-3-methylimidazolium-based ionic liquids in the presence of carbon dioxide: the influence of the ketone substituent and the ionic liquid anion on bulk electrolysis product distribution. Physical Chemistry Chemical Physics, 2015, 17, 19247-19254.	2.8	19
147	Dual Quantum Dotâ€Đecorated Bismuth Vanadate Photoanodes for Highly Efficient Solar Water Oxidation. ChemSusChem, 2019, 12, 1240-1245.	6.8	19
148	Impact of sp <sup>2</sup> Carbon Edge Effects on the Electron-Transfer Kinetics of the Ferrocene/Ferricenium Process at a Boron-Doped Diamond Electrode in an Ionic Liquid. Journal of Physical Chemistry C, 2019, 123, 17397-17406.	3.1	19
149	Voltammetric studies of polyoxometalate microparticles in contact with the reactive distillable ionic liquid DIMCARB. Electrochemistry Communications, 2005, 7, 1283-1290.	4.7	18
150	Synthesis of Metallic Nanoparticles Using Electrogenerated Reduced Forms of [l±-SiW <sub>12</sub> O <sub>40</sub> ] <sup>4–</sup> as Both Reductants and Stabilizing Agents. Chemistry of Materials, 2011, 23, 4688-4693.	6.7	18
151	Application of Bayesian Inference in Fourier-Transformed Alternating Current Voltammetry for Electrode Kinetic Mechanism Distinction. Analytical Chemistry, 2019, 91, 5303-5309.	6.5	18
152	CdSâ€Enhanced Ethanol Selectivity in Electrocatalytic CO <sub>2</sub> Reduction at Sulfideâ€Derived Cuâ^'Cd. ChemSusChem, 2021, 14, 2924-2934.	6.8	18
153	Effect of Triton X-100 on electron transfer kinetics at the interface between two immiscible electrolyte solutions: a scanning electrochemical microscopy study. Journal of Electroanalytical Chemistry, 2000, 494, 47-52.	3.8	17
154	Investigation of the kinetics of electron transfer processes involving fullerenes at liquid–liquid interfaces using scanning electrochemical microscopy: evidence for Marcus inverted region behaviour. Perkin Transactions II RSC, 2001, , 1608-1612.	1.1	17
155	Voltammetric Studies with Adhered Microparticles and the Detection of a Dependence of Organometallic Cis+→ Trans+First-Order Isomerization Rate Constants on the Identity of the Ionic Liquid. Journal of Physical Chemistry B, 2004, 108, 7363-7372.	2.6	17
156	Fourierâ€Transformed Largeâ€Amplitude AC Voltammetric Study of Tetrathiafulvalene (TTF): Electrode Kinetics of the TTF <sup>0</sup> /TTF <sup>.+</sup> and TTF <sup>.+</sup> /TTF <sup>2+</sup> Processes. ChemElectroChem, 2014, 1, 99-107.	3.4	17
157	One pot synthesis of poly(5-hydroxyl-1,4-naphthoquinone) stabilized gold nanoparticles using the monomer as the reducing agent for nonenzymatic electrochemical detection of glucose. Analytica Chimica Acta, 2015, 856, 27-34.	5.4	17
158	Ultra-small Cu nanoparticles embedded in N-doped carbon arrays for electrocatalytic CO2 reduction reaction in dimethylformamide. Nano Research, 2018, 11, 3678-3690.	10.4	17
159	The Origin of the Electrocatalytic Activity for CO <sub>2</sub> Reduction Associated with Metalâ€Organic Frameworks. ChemSusChem, 2020, 13, 2552-2556.	6.8	17
160	Designer based Fourier transformed voltammetry: A multi-frequency, variable amplitude, sinusoidal waveform. Journal of Electroanalytical Chemistry, 2009, 634, 11-21.	3.8	16
161	Electrochemical Proton Reduction and Equilibrium Acidity (p <i>K</i> <sub>a</sub> ) in Aprotic Ionic Liquids: Phenols, Carboxylic Acids, and Sulfonic Acids. Journal of Physical Chemistry C, 2015, 119, 21840-21851.	3.1	16
162	Mechanical properties of electrodeposited nanocrystalline and ultrafine-grained Zn-Sn coatings. Surface and Coatings Technology, 2018, 333, 71-80.	4.8	16

#	Article	IF	CITATIONS
163	Unique Layerâ€Dopingâ€Induced Regulation of Charge Behavior in Metalâ€Free Carbon Nitride Photoanodes for Enhanced Performance. ChemSusChem, 2020, 13, 328-333.	6.8	16
164	Electrode Material Dependence of the Electron Transfer Kinetics Associated with the [SVW11040]3â~'/4â~' (VV/IV) and [SVW11040]4â~'/5â~' (WVI/V) Processes in Dimethylformamide. Electrochimica Acta, 2016, 201, 45-56.	5.2	15
165	Electrohydrogenation of Carbon Dioxide using a Ternary Pd/Cu <sub>2</sub> O–Cu Catalyst. ChemSusChem, 2019, 12, 4471-4479.	6.8	15
166	Kinetics of bromine transfer across Langmuir monolayers of phosphatidylethanolamines at the water/air interface. Physical Chemistry Chemical Physics, 2003, 5, 3979.	2.8	14
167	Theoretical and experimental evaluation of screen-printed tubular carbon ink disposable sensor well electrodes by dc and Fourier transformed ac voltammetry. Journal of Solid State Electrochemistry, 2009, 13, 551-563.	2.5	14
168	Remarkable Sensitivity of the Electrochemical Reduction of Benzophenone to Proton Availability in Ionic Liquids. Chemistry - A European Journal, 2012, 18, 5290-5301.	3.3	14
169	Probing Electrolyte Cation Effects on the Electron Transfer Kinetics of the [α-SiW 12 O 40 ] 4â^'/5â^' and [α-SiW 12 O 40 ] 5â°'/6â^' Processes using a Boron-Doped Diamond Electrode. Electrochimica Acta, 2015, 178, 631-637.	5.2	14
170	Mixed-Metal Hybrid Polyoxometalates with Amino Acid Ligands: Electronic Versatility and Solution Properties. Inorganic Chemistry, 2016, 55, 12329-12347.	4.0	14
171	Oxomolybdate anchored on copper for electrocatalytic hydrogen production over the entire pH range. Applied Catalysis B: Environmental, 2019, 249, 227-234.	20.2	14
172	Impact of the Lithium Cation on the Voltammetry and Spectroscopy of [XVM <sub>11</sub> O <sub>40</sub> ] <sup><i>n</i>â^'</sup> (X = P, As ( <i>n</i> = 4), S ( <i>n</i> = 3); M =) T	ij <b>Ε4Ī.Q</b> q0 C	) O <b>rg</b> BT /Ove
173	Can Electrification of Ammonia Synthesis Decrease Its Carbon Footprint?. Joule, 2020, 4, 12-14.	24.0	14
174	Microelectrochemical measurements at expanding droplets (MEMED): investigation of cupric ion stripping kinetics in a two-phase oil/water system. Physical Chemistry Chemical Physics, 2000, 2, 1267-1271.	2.8	13
175	Microelectrochemical Techniques for Probing Kinetics at Liquid/Liquid Interfaces. Progress in Reaction Kinetics and Mechanism, 2004, 29, 43-166.	2.1	13
176	Systematic evaluation of electrode kinetics and impact of surface heterogeneity for surface-confined proteins using analysis of harmonic components available in sinusoidal large-amplitude Fourier transformed ac voltammetry. Analytica Chimica Acta, 2009, 652, 205-214.	5.4	13
177	Large amplitude Fourier transformed ac voltammetry at a rotating disc electrode: a versatile technique for covering Levich and flow rate insensitive regimes in a single experiment. Physical Chemistry Chemical Physics, 2012, 14, 4742.	2.8	13
178	Probing Electrode Heterogeneity Using Fourier-Transformed Alternating Current Voltammetry: Application to a Dual-Electrode Configuration. Analytical Chemistry, 2017, 89, 2830-2837.	6.5	13
179	Enhanced NADH Oxidation Using Polytyramine/Carbon Nanotube Modified Electrodes for Ethanol Biosensing. Electroanalysis, 2017, 29, 1985-1993.	2.9	13
180	Integration of Heuristic and Automated Parametrization of Three Unresolved Twoâ€Electron Surface Confined Polyoxometalate Reduction Processes by AC Voltammetry. ChemElectroChem, 2018, 5, 3771-3785.	3.4	13

#	Article	IF	CITATIONS
181	Voltammetric Studies on Decaphenylferrocene, Substituted Decaphenylferrocenes, and Their Oxidized Forms in Dichloromethane and Ionic Liquids. Organometallics, 2005, 24, 2188-2196.	2.3	12
182	Synthesis and characterization of diiron dithiolate complexes containing a quinoxaline bridge. Dalton Transactions, 2011, 40, 10907.	3.3	12
183	Effect of the N-based ligands in copper complexes for depolymerisation of lignin. New Journal of Chemistry, 2016, 40, 3511-3519.	2.8	12
184	Models and Their Limitations in the Voltammmetric Parameterization of the Sixâ€Electron Surfaceâ€Confined Reduction of [PMo <sub>12</sub> O <sub>40</sub> ] <sup>3â^'</sup> at Glassy Carbon and Boronâ€Doped Diamond Electrodes. ChemElectroChem, 2019, 6, 5499-5510.	3.4	12
185	Opportunities and challenges in applying machine learning to voltammetric mechanistic studies. Current Opinion in Electrochemistry, 2022, 34, 101009.	4.8	12
186	Efficient strategy for quality control of screen-printed carbon ink disposable sensor electrodes based on simultaneous evaluation of resistance, capacitance and Faradaic current by Fourier transform AC voltammetry. Journal of Solid State Electrochemistry, 2008, 12, 1301-1315.	2.5	11
187	A doubly amplified electrochemical immunoassay for carcinoembryonic antigen. Biosensors and Bioelectronics, 2009, 24, 1825-1830.	10.1	11
188	Metal-Templated Macrocycle Synthesis in an Ionic Liquid: A Comparison With Reaction in Protic Solvents. Synthesis and Reactivity in Inorganic, Metal Organic, and Nano Metal Chemistry, 2013, 43, 1-5.	0.6	11
189	Demonstration of Superiority of the Marcus–Hush Electrode Kinetic Model in the Electrochemistry of Dissolved Decamethylferrocene at a Gold-Modified Electrode by Fourier-Transformed Alternating Current Voltammetry. Journal of Physical Chemistry C, 2018, 122, 9009-9014.	3.1	11
190	Separating the Effects of Experimental Noise from Inherent System Variability in Voltammetry: The [Fe(CN) <sub>6</sub> ] <sup>3–/4–</sup> Process. Analytical Chemistry, 2019, 91, 1944-1953.	6.5	11
191	Lithium/bismuth co-functionalized phosphotungstic acid catalyst for promoting dinitrogen electroreduction with high Faradaic efficiency. Cell Reports Physical Science, 2021, 2, 100557.	5.6	11
192	Oxidation of 4-Methylanisole by Aqueous Cerium(IV) in a Twoâ^'Phase Immiscible Liquid/Liquid System: Interfacial versus Homogeneous Control. Journal of Physical Chemistry B, 2002, 106, 3019-3025.	2.6	10
193	Investigation of the Kinetics and Mechanism of Acid Chloride Hydrolysis in an Oil/Water System Using Microelectrochemical Measurements at Expanding Droplets (MEMED). Langmuir, 2004, 20, 1864-1870.	3.5	10
194	On choosing a reference redox system for electrochemical measurements: a cautionary tale. Journal of Solid State Electrochemistry, 2013, 17, 3021-3026.	2.5	10
195	Electrodeposition of Nanocrystalline Zinc from Sulfate and Sulfate-Gluconate Electrolytes in the Presence of Additives. Journal of the Electrochemical Society, 2016, 163, D476-D484.	2.9	10
196	Efficient Enzymatic Oxidation of Glucose Mediated by Ferrocene Covalently Attached to Polyethylenimine Stabilized Gold Nanoparticles. Electroanalysis, 2016, 28, 2728-2736.	2.9	10
197	Using Purely Sinusoidal Voltammetry for Rapid Inference of Surface-Confined Electrochemical Reaction Parameters. Analytical Chemistry, 2021, 93, 2062-2071.	6.5	10
198	Inclusion of multiple cycling of potential in the deep neural network classification of voltammetric reaction mechanisms. Faraday Discussions, 2021, 233, 44-57.	3.2	10

#	Article	IF	CITATIONS
199	Interfacial polymerisation of anilinium at Langmuir monolayers. Chemical Communications, 2004, , 450.	4.1	9
200	Room Temperature Electrodeposition of Metallic Magnesium from Ethylmagnesium Bromide in Tetrahydrofuran and Ionic Liquid Mixtures. Journal of the Electrochemical Society, 2016, 163, H3043-H3051.	2.9	9
201	Influence of Tip and Substrate Properties and Nonsteady-State Effects on Nanogap Kinetic Measurements: Response to Comment on "Impact of Adsorption on Scanning Electrochemical Microscopy Voltammetry and Implications for Nanogap Measurements― Analytical Chemistry, 2017, 89, 7273-7276.	6.5	9
202	Electrodeposition of nanocrystalline zinc‑tin alloy from aqueous electrolyte containing gluconate in the presence of polyethylene glycol and hexadecyltrimethylammonium bromide. Journal of Electroanalytical Chemistry, 2018, 813, 143-151.	3.8	9
203	Double-Layer Capacitance at Ionic Liquid–Boron-Doped Diamond Electrode Interfaces Studied by Fourier Transformed Alternating Current Voltammetry. Journal of Physical Chemistry C, 2018, 122, 11777-11788.	3.1	9
204	Spectroscopic Insights into the Mechanism of Selective Catalytic Reduction of NO by Ammonia on Sulfuric Acidâ€modified Fe 2 O 3 Surface. ChemCatChem, 2019, 11, 3035-3041.	3.7	9
205	A Comparison of Bayesian Inference Strategies for Parameterisation of Large Amplitude AC Voltammetry Derived from Total Current and Fourier Transformed Versions. ChemElectroChem, 2021, 8, 2238-2258.	3.4	9
206	Electrochemical Hydrogenation of Furfural in Aqueous Acetic Acid Media with Enhanced 2â€Methylfuran Selectivity Using CuPd Bimetallic Catalysts. Angewandte Chemie, 2022, 134, .	2.0	9
207	Theoretical Assessment of Binding and Massâ€Transport Effects in Electrochemical Affinity Biosensors That Utilize Nanoparticle Labels for Signal Amplification. Chemistry - A European Journal, 2012, 18, 15167-15177.	3.3	8
208	Influence of 1-butyl-3-methylimidazolium on the electron transfer kinetics associated with the [SVW 11 O 40 ] 3â^'/4â^' (V V/IV ) and [SVW 11 O 40 ] 4â^'/5â^' (W VI/V ) processes in dimethylformamide. Journal of Electroanalytical Chemistry, 2016, 779, 67-74.	3.8	8
209	Voltammetric Perspectives on the Acidity Scale and H <sup>+</sup> /H <sub>2</sub> Process in Ionic Liquid Media. Annual Review of Analytical Chemistry, 2018, 11, 397-419.	5.4	8
210	Radio frequency alternating electromagnetic field enhanced tetraruthenium polyoxometalate electrocatalytic water oxidation. Chemical Communications, 2019, 55, 1032-1035.	4.1	8
211	Modelling limitations encountered in the thermodynamic and electrode kinetic parameterization of the α-[S2W18O62]4â^'/5â^'/6â^' processes at glassy carbon and metal electrodes. Journal of Electroanalytical Chemistry, 2020, 872, 113786.	3.8	8
212	Thermodynamics, Electrode Kinetics, and Mechanistic Nuances Associated with the Voltammetric Reduction of Dissolved [n-Bu4N]4[PW11O39{Sn(C6H4)C≡C(C6H4)(N3C4H10)}] and a Surface-Confined Diazonium Derivative. ACS Applied Energy Materials, 2020, 3, 3991-4006.	5.1	8
213	Determination of ytterbium using electrothermal atomic absorption spectrometry with europium as chemical modifier. Analyst, The, 1995, 120, 1661.	3.5	7
214	Synthesis, characterization, crystal structure, electrochemical properties and electrocatalytic activity of an unexpected nickel(II) Schiff base complex derived from bis(acetylacetonato)nickel(II), acetone and ethylenediamine. Transition Metal Chemistry, 2014, 39, 883-891.	1.4	7
215	Reply to Comment on Stabilization of Lowâ€Valent Iron(I) in a Highâ€Valent Vanadium(V) Oxide Cluster. Angewandte Chemie - International Edition, 2019, 58, 10048-10050.	13.8	7
216	Unprecedented Formation of a Binuclear Au(II)–Au(II) Complex through Redox State Cycling: Electrochemical Interconversion of Au(I)–Au(I), Au(II)–Au(II), and Au(I)–Au(III) in Binuclear Complexes Containing the Carbanionic Ligand C6F4PPh2. Inorganic Chemistry, 2019, 58, 13999-14004.	4.0	7

#	Article	IF	CITATIONS
217	Studies on monoxide flame emission spectrometry of rare-earth elements. Part 2. Determination of yttrium in rare-earth concentrates by the dual wavelength method. Analytica Chimica Acta, 1997, 344, 291-296.	5.4	6
218	Voltammetric studies in "wet―1-butyl-1-methylpyrrolidinium bis(trifluoromethylsulfonyl)imide ionic liquid using electrodes with adhered microparticles. Electrochemistry Communications, 2012, 16, 14-18.	4.7	6
219	Investigations of Fast Electrode Kinetics for Reduction of 2,3,5,6-Tetrafluoro-7,7,8,8-tetracyanoquinodimethane in Conventional Solvents and Ionic Liquids Using Fourier Transformed Large Amplitude Alternating Current Voltammetry. Journal of Physical Chemistry C. 2014. 118, 9560-9569.	3.1	6
220	pH-Dependent solution dynamics of a manganese(ii) polyoxometalate, [Mn4(H2O)2(P2W15O56)2]16â^', and [Mn(H2O)6]2+. Dalton Transactions, 2015, 44, 19068-19071.	3.3	6
221	Probing Electrode Heterogeneity using Fourier-Transformed Alternating Current Voltammetry: Protocol Development. Electrochimica Acta, 2017, 240, 514-521.	5.2	6
222	Electrolyte cation dependence of the electron transfer kinetics associated with the [SVW11O40]3–/4– (VV/IV) and [SVW11O40]4–/5– (WVI/V) processes in propylene carbonate. Journal of Electroanalytical Chemistry, 2018, 819, 193-201.	3.8	6
223	Studies on monoxide emission spectrometry of rare-earth elements. IV. Simultaneous determination of Sm, Eu, Gd in Smî—,Euî—,Gd concentrates by the dual wavelength method. Analytica Chimica Acta, 1997, 350, 365-369.	5.4	5
224	Investigation of cupric ion extraction kinetics in a two-phase organic/water system using microelectrochemical measurements at expanding droplets (MEMED). Journal of Electroanalytical Chemistry, 2002, 538-539, 277-283.	3.8	5
225	Determination of Fast Electrode Kinetics Facilitated by Use of an Internal Reference. Analytical Chemistry, 2015, 87, 8387-8393.	6.5	5
226	Predicting <sup>17</sup> 0 NMR chemical shifts of polyoxometalates using density functional theory. Physical Chemistry Chemical Physics, 2016, 18, 8235-8241.	2.8	4
227	Size Controllable Metal Nanoparticles Anchored on Nitrogen Doped Carbon for Electrocatalytic Energy Conversion. ChemElectroChem, 2019, 6, 1508-1513.	3.4	4
228	Electrode Material Dependence, Ion Pairing, and Progressive Increase in Complexity of the α-[S <sub>2</sub> W <sub>18</sub> O <sub>62</sub> ] <sup>4â€"/5â€"/6â€"/7â€"/8â€"/9â€"/10â€"</sup> Red Processes in Acetonitrile Containing [ <i>n</i> Bu <sub>4</sub> N][PF <sub>6</sub> ] as the Supporting Electrolyte. Journal of Physical Chemistry C, 2020, 124, 16032-16047.	uction	4
229	Studies on monoxide emission spectrometry of rare earth elementsPart V.†Determination of Dy in rare earth concentrates by dual wavelength method. Analyst, The, 1998, 123, 1235-1238.	3.5	3
230	A Systematic Study of the Mass Transport, Kinetic and Thermodynamic Properties of the FeIII/II Process at Glassy Carbon and Boron-Doped Diamond Electrodes. Electrochimica Acta, 2017, 249, 421-430.	5.2	3
231	Changing the Action of Iron from Stoichiometric to Electrocatalytic in the Hydrogenation of Ketones in Aqueous Acidic Media. ChemSusChem, 2015, 8, 3712-3717.	6.8	2
232	A Facile Chemicalâ€Free and Universal Method for Transfer of Ultrathin Grapheneâ€Based Films. Advanced Materials Interfaces, 2016, 3, 1600540.	3.7	2
233	Chapter 7. Electrocarboxylation in Ionic Liquids. RSC Energy and Environment Series, 2018, , 160-181.	0.5	2
234	Ultraâ€ŧhin Pd and CuPd Bimetallic Alloy Nanosheets for Electrochemical Reduction of CO <sub>2</sub> . ChemElectroChem, 2022, 9, .	3.4	2

Jie Zhang

#	Article	IF	CITATIONS
235	TiO <sub>2</sub> nanocrystal rods on titanium microwires: growth, vacuum annealing, and photoelectrochemical oxygen evolution. New Journal of Chemistry, 2022, 46, 8385-8392.	2.8	2
236	Investigation of Molecular Transfer Processes across Phospholipid Monolayers by the Combined Scanning Electrochemical Microscopy-Langmuir Trough Technique. Progress in Reaction Kinetics and Mechanism, 2007, 32, 195-217.	2.1	1
237	Additions and corrections for Journal of Materials Chemistry C published 12th March 2014 to 25th June 2014. Journal of Materials Chemistry C, 2014, 2, 6879.	5.5	1
238	Electroanalytical Applications of Semiintegral and Convolution Voltammetry in Room-Temperature Ionic Liquids. , 2015, , 143-167.		1
239	Variation of Carbon Based Materials on the Electropolymerization of Tyramine. Electroanalysis, 2018, 30, 1545-1555.	2.9	1
240	Identification of Mechanistic Subtleties that Apply to Voltammetric Studies at Boron-Doped Diamond Electrodes. Journal of Physical Chemistry C, 2020, 124, 24232-24244.	3.1	1
241	Modeling the Influence of Low Concentrations of Water on the Thermodynamics, Electron Transfer Kinetics, and Diffusivity of the [Ru(CN)6]4–/3– Process in Propylene Carbonate. Journal of Physical Chemistry C, 2020, 124, 13726-13738.	3.1	1
242	Voltammetry of Adhered Microparticles in Contact with Ionic Liquids: Principles and Applications. , 2015, , 405-433.		0
243	Synergistic Functionalization for Promoting Dinitrogen Electroreduction with High Faradaic Efficiency. SSRN Electronic Journal, 0, , .	0.4	0